NIH Public Access
Author Manuscript
Mol Cancer Ther. Author manuscript; available in PMC 2014 November 01.

Published in final edited form as:
Mol Cancer Ther. 2013 November ; 12(11): . doi:10.1158/1535-7163.MCT-13-0284.

Hsp90 inhibitors promote p53-dependent apoptosis through PUMA and Bax

Kan He[#1,3], **Xingnan Zheng**[#1,3], **Lin Zhang**[2,3], and **Jian Yu**[1,3,&]

[1]Department of Pathology, University of Pittsburgh School of Medicine, 5117 Centre Ave., Pittsburgh, PA 15213, USA.

[2]Department of Pharmacology and Chemical Biology, University of Pittsburgh School of Medicine, 5117 Centre Ave., Pittsburgh, PA 15213, USA.

[3]University of Pittsburgh Cancer Institute 5117 Centre Ave., Pittsburgh, PA 15213, USA.

[#] These authors contributed equally to this work.

Abstract

Heat shock protein 90 (Hsp90) is widely overexpressed in cancer cells and believed to be essential for the maintenance of malignant phenotypes. Targeting Hsp90 by small molecules has shown promises in solid and hematological malignancies, which likely involves degradation of client oncoproteins in a cell-type specific manner. In this study, we found that structurally unrelated Hsp90 inhibitors induce DNA damage and apoptosis via p53-dependent induction of PUMA, which indirectly triggers Bax activation and mitochondrial dysfunction in colon cancer cells. Deficiency in *PUMA, BAX,* or *p53* at lesser extent, abrogated 17AAG-induced apoptosis and mitochondrial dysfunction, and enhanced clonogenic cell survival. Furthermore, suppression of p53-dependent p21 induction or enhanced p53 activation synergized with 17AAG to induce *PUMA*-dependent apoptosis. Finally, PUMA was found to mediate apoptotic and therapeutic responses to the 17AAG analog 17DMAG in xenografts. These results demonstrate an important role of the p53/PUMA/Bax axis in Hsp90 inhibitor-induced killing of p53 WT cells, and have important implications for their clinical applications.

Keywords

Hsp90 inhibitors; PUMA; p53; apoptosis; colon cancer

Introduction

Heat shock protein 90 (Hsp90) is one of the most abundant molecular chaperones in eukaryotes and regulates many cellular processes including signal transduction, protein degradation, protein folding and maturation of client proteins (1). Over 200 proteins have been reported to be Hsp90 clients, including many oncogenic proteins, such as mutant p53, Raf-1, Akt (1-2), and others associated with hallmarks of cancer (3). Interestingly, Hsp90 is constitutively expressed at 2–10-fold higher levels in tumor cells than their normal

[&]**Correspondence:** Jian Yu, Ph.D., Hillman Cancer Center Research Pavilion, Suite 2.26h, 5117 Centre Ave, Pittsburgh, PA 15213. yuj2@upmc.edu; Phone: 412-623-7786; Fax: 412-623-7778.

Disclosures: All authors disclosed no conflict of interest, and agreed on the submission.

Author contributions:
JY conceived and supervised the study. KH, XZ and JY designed experiments, analyzed and interpreted data, and wrote the paper. KH and XZ performed experiments. LZ designed experiments and analyzed data.

NIH-PA Author Manuscript
NIH-PA Author Manuscript
NIH-PA Author Manuscript

NIH-PA Author Manuscript

NIH-PA Author Manuscript

NIH-PA Author Manuscript

counterparts (4), and appears to be required for malignant transformation (5), and a selective therapeutic target in cancer cells (1-2). Hsp90 targeting has attracted considerable attention since the late 1990s. Currently, over 17 Hsp90 inhibitors have entered clinical trials as potential anticancer agents (1, 5). These inhibitors, such as the natural product geldanamycin (GA) and its less toxic analog 17-allylamino-17-demethoxygeldanamycin (17AAG) inhibit the molecular chaperone function of Hsp90 by binding to its ATP/ADP pocket and causing destabilization of its complexes with client proteins (2). Treatment with GA and 17AAG can induce apoptosis, inhibit metastasis or angiogenesis in both cell and animal models (1, 5-6). 17AAG is one of the very first Hsp90 inhibitors to complete phase II clinical trials (1, 5). Other Hsp90 inhibitors with improved pharmaceutical properties, such as 17DMAG and NVPAUY922, can promote apoptosis in preclinical models and are currently in phase I/II clinical trials (1, 7). However, the mechanisms underlying Hsp90 inhibition-induced cell killing are currently not well understood, and may vary by cell type. Several mechanisms have been suggested, including Akt down-regulation (8), inhibition of NF-κB activation due to IKK destabilization (9), ER stress (10), and more recently p53 activation (11-12).

The Bcl-2 family proteins are the central regulators of mitochondria-mediated apoptosis (13-15). The BH3-only sub family members are proximal signaling molecules that respond to distinct as well as overlapping signals, and consist of at least 10 members. Several of BH3-only proteins, such as PUMA and Bim, activate Bax/Bak following the neutralization of all known anti-apoptotic Bcl-2 family members (13-15) to promote mitochondrial dysfunction and caspase activation (16-18). PUMA is a critical mediator of p53-dependent and -independent apoptosis in multiple tissues and cell types (18). Transcription of PUMA is mainly dependent on p53 activity in response to DNA-damaging agents such as γ-irradiation, common chemotherapeutic drugs (18-19), and even some kinase inhibitors (20). Upon exposure to non-genotoxic stimuli, PUMA is induced by other transcriptional factors such as p73 (21-22), NF-κB (23), and FoxO3a (24-25). Bim regulates apoptosis in immune cells, normal and malignant hematopoietic cells, and some epithelial cells generally following nongenotoxic stresses (13).

In this study, we investigated the mechanisms of apoptosis induced by Hsp90 inhibitors in colon cancer cells. We found that p53-mediated induction of PUMA and Bax is required for the apoptotic responses to Hsp90 inhibitors via the mitochondrial pathway *in vitro* and *in vivo*. In contrast, p53-mediated p21 induction suppresses 17AAG-induced apoptosis. Enhanced p53 activation or p21 inhibition sensitized p53 WT colon cancer cells to *PUMA*-dependent apoptosis following treatment with Hsp90 inhibitors. These results demonstrate an important role of the p53/PUMA/Bax axis in the therapeutic responses to Hsp90 inhibitors in p53 WT cancers, and have important implications for their future development and applications.

Materials and Methods

Cell culture and treatment

The human colorectal cancer cell lines, including HCT116, RKO, LoVo (wild-type (WT) p53, HT29 and DLD1 (mutant *p53*), were obtained from the American Type Culture Collection (Manassas, VA, USA). Isogenic HCT 116 knockout cell lines including *p53*-KO (26), *PUMA*-KO (27), *BAX*-KO (28), *p21*-KO (29), *p21*/*PUMA*- double KO (27) and *PUMA*-KO DLD1 cells (30) have been described. We examine loss of expression of targeted proteins by western blotting and conduct Mycoplasma testing by PCR during culture routinely. No additional authentication was done by the authors. Details on cell culture and drug treatments are found in the supplemental materials.

NIH-PA Author Manuscript

NIH-PA Author Manuscript

NIH-PA Author Manuscript

Western blotting

Western blotting was performed as previously described (16). More details on antibodies are found in the supplemental materials.

Real-time Reverse Transcriptase (RT) PCR

Total RNA was isolated from 17AAG-treated cells using the Mini RNA Isolation II Kit (Zymo Research, Orange, CA) according to the manufacturer's protocol. One μg of total RNA was used to generate cDNA using SuperScript II reverse transcriptase (Invitrogen, Carlsbad, CA, USA). Real-time PCR was carried out as before (24). Details on primers are found in the supplemental materials.

Small-interfering RNA knockdown

Transfection was performed 24 hours before 17AAG treatment using 400 pmol of siRNA in one well of a 12-well plate (20). All siRNA, including FoxO3a (ON-TARGETplus J-003007-10), PUMA (ACGTGTGACCACTGGCATTdTdT, and ACCTCAACGCACAGTACGAdTdT) (31), and Bim (GACCGAGAAGGUAGACAAUdTdT) (32) were synthesized by Dharmacon (Lafayette, CO, USA), and siRNAs were transfected with lipofectamine 2000 (Invitrogen, Carlsbad, CA, USA) according to the manufacturer's instructions.

Luciferase assays

PUMA luciferase reporter constructs (Fragments A-E) have been described previously (22). For reporter assays, cells were transfected with the fragment *PUMA* reporter along with the transfection control β-galactosidase reporter pCMVβ (Promega, Madison, WI, USA). Cell lysates were collected and luciferase activities were measured as previously described (33). All reporter experiments were performed in triplicate and repeated three times.

Analysis of apoptosis and cell death

Apoptosis was analyzed by nuclear staining with Hoechst 33258 (Invitrogen), and Annexin V/propidium iodide (PI) (Invitrogen) followed by flow cytometry as described (30). For colony formation assays, the same number of cells were treated and plated in 12-well plates at appropriate dilutions, and allowed to grow for 10–14 days before staining with crystal violet (Sigma, St. Louis, MO). For detection of mitochondrial membrane potential change, the treated cells were stained by JC-1 (30001, Biotium, Hayward, CA, USA) for 15 minutes according to the manufacturer's instruction, and then analyzed by flow cytometry.

Analysis of cytochrome c release and Bax multimerization, conformational change and interacting proteins

Cytoplasmic and mitochondrial fractions were separated by Mitochondrial Fractionation Kit (Active Motif, Carlsbad, CA, USA) according to the manufacturer's instructions. Cytochrome c in both cytoplasmic and mitochondrial fractions was detected by Western blotting. To detect Bax multimerization, purified mitochondrial fractions were cross-linked with 1mM of Dithiobis (succinimidyl) propionate (DSP) (Pierce, Rockford, IL, USA) as described (34-35), followed by Western blotting under non-denaturing conditions. Methods on detection of Bax conformational change (27) and interacting protein (16) have been described and details are found in the supplemental materials.

Xenograft studies

All animal experiments were approved by the University of Pittsburgh Institutional Animal Care and Use Committee. Female 5–6 week-old Nu/Nu mice (Charles River, Wilmington,

NIH-PA Author Manuscript

NIH-PA Author Manuscript

NIH-PA Author Manuscript

MA) were housed in a sterile environment with micro isolator cages and allowed access to water and chow *ad libitum*. Mice were injected subcutaneously in both flanks with 4×10^6 WT or *PUMA*-KO HCT116 cells. After implantation, tumors were allowed to grow 7 days before treatment was initiated. Mice were randomized into two groups (n = 6 per group) receiving either vehicle (saline) or 17DMAG (15mg/kg/d) on days 1-4 and 7-11, respectively (36). Detailed methods on tumor measurements, harvests and histological analysis are found in the supplemental materials and as described (24, 31).

Statistical Analysis

Statistical analyses were carried out using GraphPad Prism IV software. P values were calculated by the student's t-test and were considered significant if $p < 0.05$. The means ± one standard deviation (s.d.) are displayed in the figures.

Results

p53-dependent induction of PUMA and Bax by 17AAG in colon cancer cells

To determine a potential role of the Bcl-2 family in Hsp90 inhibitor-induced apoptosis, we first examined protein levels of its major members following 17AAG treatment in HCT116 colon cancer cells (Fig. 1A). Among them, PUMA, Bim and Bax were significantly induced, and induction was detected as early as 24 hours after treatment (Fig 1A). The levels of *PUMA, BIM* and *BAX* transcripts were also elevated (Fig. 1B). The expression of other Bcl-2 family members such as Bid, Bcl-2, and Bcl-xL remained unchanged, while that of Noxa and Mcl-1 decreased (Fig. 1A). We then treated parental, and *p53*-KO HCT116 or RKO cells with 17AAG to determine whether p53 is involved in the induction of PUMA, Bim and Bax. Induction of PUMA and Bax, but not Bim, was largely blocked in *p53*-KO cells, compared to parental cells (Fig 1C). Furthermore, we used a series of *PUMA* promoter luciferase reporters (containing ~2 kb upstream from the transcriptional initiation site) (22) to determine whether p53 directly activates *PUMA* transcription. We found that the reporters containing the two p53 binding sites (Frag “A”and “E”) had much higher activities after 17AAG treatment in *p53* WT cells than in *p53*-KO HCT 116 cells (Fig. 1D). Moreover, the induction of PUMA and other p53 targets Bax and p21 paralleled that of p53, p53S15 phosphorylation and γ-H2AX, a marker of DNA double-strand breaks (Fig. 1E). Consistent with reports in other systems (37-38), 17AAG treatment decreased AKT and p-ERK (Fig. S1.). These findings demonstrate that 17AAG treatment leads to p53-dependent induction of PUMA and Bax, besides modulation of survival pathways.

PUMA mediates Hsp90 inhibitor-induced apoptosis

To examine a potential role of PUMA in 17AAG-induced apoptosis, we compared the responses of parental HCT116 cells with isogenic *PUMA* knockout (*PUMA*-KO) cells (27). 17AAG treatment induced apoptosis in HCT116 cells as early as 24 hours, which increased to over 30% at 72 hours, while apoptosis and activation of caspase-3 and -9 were abolished in *PUMA*-KO cells (Fig. 2A). Annexin V/propidium iodide staining confirmed apoptotic resistance of *PUMA*-KO cells (Fig. S2A and S2B). *PUMA*-KO cells were also found to be significantly more resistant to 17AAG than WT cells in a long-term clonogenic assay (Fig. 2B). *PUMA* knockdown suppressed 17AAG-induced apoptosis in *p53* WT cell lines LoVo and RKO (Fig. 2C). In contrast, *BIM* knockdown did not inhibit 17AAG-induced apoptosis (Figs. S2C, S2D). Furthermore, 17DMAG and NVPAUY922 induced significant apoptosis in HCT 116 cells, which was largely blocked in *PUMA*-KO cells (Figs. 2D and S3). Collectively, these results indicate that PUMA is required for Hsp90 inhibitor-induced apoptosis in colon cancer cells with WT p53.

NIH-PA Author Manuscript

NIH-PA Author Manuscript

NIH-PA Author Manuscript

PUMA mediates 17AAG-induced apoptosis via the mitochondrial pathway and Bax activation

17AAG-induced apoptosis in HCT 116 was associated with mitochondrial membrane depolarization and release of cytochrome c and SMAC, which was suppressed in *PUMA*-KO cells (Fig. 3A). 17AAG treatment also induced PUMA-dependent Bax conformational changes and oligomerization (Fig. 3B and 3C). *BAX*-KO HCT116 cells were found to be resistant to 17AAG-induced apoptosis, and activation of caspase-3 and -9 (Fig. 3D), consistent with PUMA acting upstream of Bax (13-15). We further probed interactions of Bax with several Bcl-2 family members. 17AAG treatment induced dissociation of Bax from Bcl-xL and Bcl-2, which was suppressed in *PUMA* KO cells (Fig. 3E). In contrast, Bmi binding to Bax was largely unaffected by *PUMA* status or 17AAG treatment. No interaction was detected between Bax and Mcl-1, PUMA or Noxa. Interestingly, levels of Mcl-1 and Noxa decreased significantly upon 17AAG treatment in HCT 116 cells, which was reduced in *PUMA* KO cells (Figs. 1A and Fig. 3E). These results demonstrate that PUMA functions upstream of Bax to induce Bax activation and mitochondrial dysfunction in17AAG-induced apoptosis. PUMA likely activates Bax indirectly by replacing it from Bcl-xL or Bcl-2 (16, 39), and altered interactions among Bcl-2 family might affect their stabilities.

p53-dependent p21 induction inhibits 17AAG-induced apoptosis

p21 also showed *p53*-dependent induction following 17AAG treatment, while *p53*-KO cells were less resistant than *PUMA*-KO to 17AAG-induced apoptosis (Figs. 1E, 4A, 4B and S4). We hypothesized that p21-induction might inhibit apoptosis induced by Hsp90 inhibitors, much like it inhibits apoptosis induced by DNA damage (40-41). Indeed, *p21*-KO HCT 116 cells were found to be more sensitive to 17AAG-induced apoptosis compared to parental cells. Apoptosis was significantly reduced in *p21/PUMA* double KO (DKO) cells that phenocopied *p53*-KO cells (Figs. 4B and S4). UCN-01 was shown to selectively block p53 phosphorylation on S20 but not S15 by targeting Chk1 after DNA damage (42-43). We found that UCN-01 eliminated p21 expression and significantly enhanced 17AAG-induced apoptosis (Fig. 4C). The apoptosis induced by 17AAG and UCN-01 combination was partially dependent on *PUMA* (Fig. 4D). Together, these data suggest that p53-dependent induction of p21 suppresses the apoptotic response to 17AAG, and selective inhibition of p21 while preserving PUMA induction enhances cell killing.

Enhanced p53 activity synergizes with 17AAG to induce PUMA-dependent apoptosis

Chemosensitization effects of 17AAG have been extensively documented (1, 7). We found that HCT116 cells were relatively resistant to Cisplatin-induced apoptosis or PUMA expression, while p53 stabilization and serine 15 (S15) phosphorylation were readily detected (Fig. 5A and 5B). The combination of 17AAG with Cisplatin synergistically induced apoptosis, caspase activation, and PUMA expression in HCT 116 cells (Fig. 5A and 5B). The combination of 17AAG with Nutlin-3, a p53 activator that disrupts MDM2/MDMX and p53 interactions, also synergistically induced apoptosis and PUMA induction (Fig. 5C and 5D). Remarkably, the combination treatment-induced apoptosis was almost completely abolished in *PUMA*-KO cells (Fig. 5A and 5C). PUMA induction was reduced in *p53*-KO cells compared to WT HCT 116 cells (Fig. 5B and 5D). Loss of p21 induction likely explains why *p53*-KO cells were more sensitive than *PUMA*-KO to apoptosis induced by these combinations (Figs. 5A and 5B and S5). In addition, *p53*-KO cells were also partially resistant to apoptosis induced by 17DMAG and NVP-AUY922, and showed significantly reduced induction of PUMA and Bax, but not Bim (Fig. S5). These data demonstrate a general role of the p53/PUMA/Bax axis in Hsp90 inhibitor-induced apoptosis and chemosensitization in colon cancer cells.

NIH-PA Author Manuscript

NIH-PA Author Manuscript

NIH-PA Author Manuscript

Anti-tumor activities of Hsp90 inhibitors is mediated by PUMA-dependent apoptosis *in vivo*

To determine whether PUMA-mediated apoptosis plays a critical role in the anti-tumor activities of Hsp90 inhibitors *in vivo*, we established WT and *PUMA*-KO HCT116 xenograft tumors in nude mice. Tumor bearing mice were then treated with 15 mg/kg 17DMAG, which is water-soluble, or the vehicle by i.p., and tumor volumes were monitored every two days for 3 weeks. The WT tumors, but not *PUMA*-KO HCT116 tumors, responded well to 17DMAG treatment and reached roughly 1/4 the size of the tumors in vehicle treated mice on day 21 (Fig. 6A). PUMA, Bax, Bim as well as p53 phosphorylation (S15) were significantly induced by 17DMAG treatment in WT tumors (Fig. 6B), consistent with our *in vitro* data. TUNEL and active caspase-3 staining revealed marked apoptosis in these tumors, which decreased by over 55% in the *PUMA*-KO tumors treated identically (Fig. 6C and 6D). These data demonstrated an important role of the p53/PUMA/Bax axis in the anti-tumor activities of 17DMAG *in vivo.*

Discussion

Hsp90 helps mammalian cells and lower eukaryotes to cope with environmental stresses (44). Cancer cells are constantly under a variety of stresses (3) and Hsp90 is believed to help buffer such stresses for their survival, while different client proteins might be involved depending on cellular context (1, 7). Hsp90 inhibitors induce apoptosis in a variety of preclinical models through degradation of oncogenic client proteins including mutant p53, Raf-1, Akt, Her-2 and ALK fusion proteins (1, 7, 45). Using multiple cell lines and structurally unrelated compounds, we demonstrate a role of the p53/PUMA/Bax axis in Hsp90 inhibitor-induced apoptosis and chemosensitization in colon cancer cells using cell culture and xenograft models. p53-dependent PUMA expression directly activates Bax and the mitochondrial apoptotic pathway. Modulation of other Bcl-2 family members and survival pathways (37-38), and ER stress (Fig. S6) can also contribute to apoptosis or PUMA induction. However, the cell killing mechanisms by Hsp90 inhibitors are likely different in *p53* WT and mutant cancer cells where mutant p53 is targeted for degradation (46-48).

Several recent studies showed that functional p53 is required for the induction of apoptosis by 17AAG (11-12), while the mechanism has not been well defined. We discovered distinct roles of p53-mediated PUMA and p21 induction in this process. In contrast to p53-mediated induction of PUMA/Bax, induction of p21 protected against 17AAG-induced apoptosis, consistent with the known antiapoptotic function of p21 in p53-dependent apoptosis (40-41). The induction of γ-H2AX further suggests a classical p53-dependent DNA damage response associated with double strand breaks (Fig 1E) (40-41, 49), while the precise cause of DNA damage upon Hsp90 inhibition remains to be defined. 17AAG is commonly used as a chemosensitizer and enhances cell killing when combined with a variety of cytotoxic agents, such as cisplatin, UCN-01, taxol, gemcitabine, cytarabine, or proteasome inhibitors and HDAC inhibitors (7). Our results provide mechanistic insights for such a synergy in p53 WT cells. For examples, Cisplatin or Nutlin-3 enhances 17AAG-induced cell killing via enhanced p53 activity and PUMA/Bax induction. On the other hand, UCN-01 enhances 17AAG-induced cell killing by blocking p21 expression. Therefore, selective modulation of p53-mediated apoptosis or cell cycle arrest can be exploited to enhance cancer cell killing.

The results of Hsp90 inhibitors in clinical trials are mixed (1, 5), likely reflecting lack of patient stratification or biomarkers. Improved response rates were observed in HER2-positive metastatic breast cancer patients treated with 17AAG and trastuzumab (50), as well as in ALK-rearranged non-small cell lung cancer (NSCLC) patients treated with Hsp90 inhibitor IPI-504 (51). This has been attributed to the degradation of the Hsp90 clients as

NIH-PA Author Manuscript

NIH-PA Author Manuscript

NIH-PA Author Manuscript

driver oncoproteins. Our study together with others (11-12) would strongly suggests that this class of agents works differently in cancers with WT *p53*, and examining the modulation of PUMA, Bax, Bim, and p21 might help better distinguish responders from non-responders in these tumors. No mutation in the *PUMA* gene has been reported in human cancer while reduced PUMA expression has been reported in cutanous melanoma and Burkitt's lymphomas (18). Therefore reduced PUMA expression can potentially contribute to resistance to Hsp90 inhibitors. Toxicity to normal tissues is also a concern of Hsp90 inhibitors. It is tempting to speculate that blocking p53-dependent apoptosis might selectively reduce normal tissue toxicity without compromising efficacy in tumors harboring mutant *p53*.

In conclusion, we have shown that the p53/PUMA/Bax axis plays an important role in the therapeutic and apoptotic response to Hsp90 inhibitors in p53WT cancer cells. Loss of *PUMA, BAX*, or *p53* leads to resistance at varying degrees, while loss of *p21* leads to sensitization. These findings provide novel mechanistic insights for Hsp90 inhibitor-induced apoptosis, and can have important implications for their future development and application.

Supplementary Material

Refer to Web version on PubMed Central for supplementary material.

Acknowledgments

We thank Bert Vogelstein (Howard Hughes Medical Institute, Johns Hopkins University) for *p53*-KO, *p21*-KO HCT116 cells, and *p53*-KO RKO cells, and other members of Yu and Zhang laboratories for helpful discussions.

Financial information

This work is supported by NIH grant CA129829, American Cancer Society grant RGS-10-124-01-CCE, FAMRI (J. Yu), and by NIH grants CA106348, CA121105, and American Cancer Society grant RSG-07-156-01-CNE (L. Zhang). This project used shared facilities that were supported in part by UPCI CCSG award P30CA047904.

References

1. Neckers L, Workman P. Hsp90 molecular chaperone inhibitors: are we there yet? Clin Cancer Res. 2012; 18:64–76. [PubMed: 22215907]
2. Kamal A, Thao L, Sensintaffar J, Zhang L, Boehm MF, Fritz LC, et al. A high-affinity conformation of Hsp90 confers tumour selectivity on Hsp90 inhibitors. Nature. 2003; 425:407–10. [PubMed: 14508491]
3. Hanahan D, Weinberg RA. Hallmarks of cancer: the next generation. Cell. 2011; 144:646–74. [PubMed: 21376230]
4. Ferrarini M, Heltai S, Zocchi MR, Rugarli C. Unusual expression and localization of heat-shock proteins in human tumor cells. International journal of cancer Journal international du cancer. 1992; 51:613–9. [PubMed: 1601523]
5. Workman P, Burrows F, Neckers L, Rosen N. Drugging the cancer chaperone HSP90: combinatorial therapeutic exploitation of oncogene addiction and tumor stress. Ann N Y Acad Sci. 2007; 1113:202–16. [PubMed: 17513464]
6. Hostein I, Robertson D, DiStefano F, Workman P, Clarke PA. Inhibition of signal transduction by the Hsp90 inhibitor 17-allylamino-17-demethoxygeldanamycin results in cytostasis and apoptosis. Cancer research. 2001; 61:4003–9. [PubMed: 11358818]
7. Lu X, Xiao L, Wang L, Ruden DM. Hsp90 inhibitors and drug resistance in cancer: the potential benefits of combination therapies of Hsp90 inhibitors and other anti-cancer drugs. Biochem Pharmacol. 2012; 83:995–1004. [PubMed: 22120678]

NIH-PA Author Manuscript

NIH-PA Author Manuscript

NIH-PA Author Manuscript

8. Munster PN, Marchion DC, Basso AD, Rosen N. Degradation of HER2 by ansamycins induces growth arrest and apoptosis in cells with HER2 overexpression via a HER3, phosphatidylinositol 3'-kinase-AKT-dependent pathway. Cancer research. 2002; 62:3132–7. [PubMed: 12036925]
9. Rakitina TV, Vasilevskaya IA, O'Dwyer PJ. Additive interaction of oxaliplatin and 17-allylamino-17-demethoxygeldanamycin in colon cancer cell lines results from inhibition of nuclear factor kappaB signaling. Cancer research. 2003; 63:8600–5. [PubMed: 14695170]
10. Davenport EL, Moore HE, Dunlop AS, Sharp SY, Workman P, Morgan GJ, et al. Heat shock protein inhibition is associated with activation of the unfolded protein response pathway in myeloma plasma cells. Blood. 2007; 110:2641–9. [PubMed: 17525289]
11. Ayrault O, Godeny MD, Dillon C, Zindy F, Fitzgerald P, Roussel MF, et al. Inhibition of Hsp90 via 17-DMAG induces apoptosis in a p53-dependent manner to prevent medulloblastoma. Proceedings of the National Academy of Sciences of the United States of America. 2009; 106:17037–42. [PubMed: 19805107]
12. Vaseva AV, Yallowitz AR, Marchenko ND, Xu S, Moll UM. Blockade of Hsp90 by 17AAG antagonizes MDMX and synergizes with Nutlin to induce p53-mediated apoptosis in solid tumors. Cell death & disease. 2011; 2:e156. [PubMed: 21562588]
13. Youle RJ, Strasser A. The BCL-2 protein family: opposing activities that mediate cell death. Nat Rev Mol Cell Bio. 2008; 9:47–59. [PubMed: 18097445]
14. Yu J, Zhang L. Apoptosis in human cancer cells. Curr Opin Oncol. 2004; 16:19–24. [PubMed: 14685088]
15. Leibowitz B, Yu J. Mitochondrial signaling in cell death via the Bcl-2 family. Cancer Biol Ther. 2010; 9:417–22. [PubMed: 20190564]
16. Ming L, Wang P, Bank A, Yu J, Zhang L. PUMA dissociates Bax and BCL-XL to induce apoptosis in colon cancer cells. J Biol Chem. 2006; 281:16034–42. [PubMed: 16608847]
17. Yu J, Wang P, Ming L, Wood MA, Zhang L. SMAC/Diablo mediates the proapoptotic function of PUMA by regulating PUMA-induced mitochondrial events. Oncogene. 2007; 26:4189–98. [PubMed: 17237824]
18. Yu J, Zhang L. PUMA, a potent killer with or without p53. Oncogene. 2008; 27(Suppl 1):S71–83. [PubMed: 19641508]
19. Yu J, Zhang L. No PUMA, no death: implications for p53-dependent apoptosis. Cancer Cell. 2003; 4:248–9. [PubMed: 14585351]
20. Zheng X, He K, Zhang L, Yu J. Crizotinib induces PUMA-dependent apoptosis in colon cancer cells. Mol Cancer Ther. 2013; 12:777–86. [PubMed: 23427294]
21. Melino G, Bernassola F, Ranalli M, Yee K, Zong WX, Corazzari M, et al. p73 Induces apoptosis via PUMA transactivation and Bax mitochondrial translocation. J Biol Chem. 2004; 279:8076–83. [PubMed: 14634023]
22. Ming L, Sakaida T, Yue W, Jha A, Zhang L, Yu J. Sp1 and p73 activate PUMA following serum starvation. Carcinogenesis. 2008; 29:1878–84. [PubMed: 18579560]
23. Wang P, Qiu W, Dudgeon C, Liu H, Huang C, Zambetti GP, et al. PUMA is directly activated by NF-kappa B and contributes to TNF-alpha-induced apoptosis. Cell Death Differ. 2009; 16:1192–202. [PubMed: 19444283]
24. Dudgeon C, Wang P, Sun X, Peng R, Sun Q, Yu J, et al. PUMA induction by FoxO3a mediates the anticancer activities of the broad-range kinase inhibitor UCN-01. Molecular cancer therapeutics. 2010; 9:2893–902. [PubMed: 20978166]
25. Sun J, Sun Q, Brown MF, Dudgeon C, Chandler J, Xu X, et al. The Multi-Targeted Kinase Inhibitor Sunitinib Induces Apoptosis in Colon Cancer Cells via PUMA. PLoS One. 2012; 7:e43158. [PubMed: 22912816]
26. Bunz F, Hwang PM, Torrance C, Waldman T, Zhang Y, Dillehay L, et al. Disruption of p53 in human cancer cells alters the responses to therapeutic agents. The Journal of clinical investigation. 1999; 104:263–9. [PubMed: 10430607]
27. Yu J, Wang Z, Kinzler KW, Vogelstein B, Zhang L. PUMA mediates the apoptotic response to p53 in colorectal cancer cells. Proceedings of the National Academy of Sciences of the United States of America. 2003; 100:1931–6. [PubMed: 12574499]

NIH-PA Author Manuscript

NIH-PA Author Manuscript

NIH-PA Author Manuscript

28. Zhang L, Yu J, Park BH, Kinzler KW, Vogelstein B. Role of BAX in the apoptotic response to anticancer agents. Science. 2000; 290:989–92. [PubMed: 11062132]
29. Waldman T, Kinzler KW, Vogelstein B. p21 Is Necessary For the p53-Mediated G(1) Arrest In Human Cancer Cells. Cancer Res. 1995; 55:5187–90. [PubMed: 7585571]
30. Wang P, Yu J, Zhang L. The nuclear function of p53 is required for PUMA-mediated apoptosis induced by DNA damage. Proceedings of the National Academy of Sciences of the United States of America. 2007; 104:4054–9. [PubMed: 17360476]
31. Sun Q, Ming L, Thomas SM, Wang Y, Chen ZG, Ferris RL, et al. PUMA mediates EGFR tyrosine kinase inhibitor-induced apoptosis in head and neck cancer cells. Oncogene. 2009; 28:2348–57. [PubMed: 19421143]
32. Han J, Goldstein LA, Gastman BR, Rabinowich H. Interrelated roles for Mcl-1 and BIM in regulation of TRAIL-mediated mitochondrial apoptosis. The Journal of biological chemistry. 2006; 281:10153–63. [PubMed: 16478725]
33. Yu J, Zhang L, Hwang PM, Kinzler KW, Vogelstein B. PUMA induces the rapid apoptosis of colorectal cancer cells. Molecular cell. 2001; 7:673–82. [PubMed: 11463391]
34. Wu B, Qiu W, Wang P, Yu H, Cheng T, Zambetti GP, et al. p53 independent induction of PUMA mediates intestinal apoptosis in response to ischaemia-reperfusion. Gut. 2007; 56:645–54. [PubMed: 17127703]
35. Qiu W, Carson-Walter EB, Liu H, Epperly M, Greenberger JS, Zambetti GP, et al. PUMA regulates intestinal progenitor cell radiosensitivity and gastrointestinal syndrome. Cell Stem Cell. 2008; 2:576–83. [PubMed: 18522850]
36. Moser C, Lang SA, Kainz S, Gaumann A, Fichtner-Feigl S, Koehl GE, et al. Blocking heat shock protein-90 inhibits the invasive properties and hepatic growth of human colon cancer cells and improves the efficacy of oxaliplatin in p53-deficient colon cancer tumors in vivo. Molecular cancer therapeutics. 2007; 6:2868–78. [PubMed: 18025273]
37. Sato S, Fujita N, Tsuruo T. Modulation of Akt kinase activity by binding to Hsp90. Proceedings of the National Academy of Sciences of the United States of America. 2000; 97:10832–7. [PubMed: 10995457]
38. Jia WT, Yu CR, Rahmani M, Krystal G, Sausville EA, Dent P, et al. Synergistic antileukemic interactions between 17-AAG and UCN-01 involve interruption of RAF/MEK- and AKT-related pathways. Blood. 2003; 102:1824–32. [PubMed: 12738674]
39. Peng R, Tong JS, Li H, Yue B, Zou F, Yu J, et al. Targeting Bax interaction sites reveals that only homo-oligomerization sites are essential for its activation. Cell Death Differ. 2013; 20:744–54. [PubMed: 23392123]
40. Yu J, Zhang L. The transcriptional targets of p53 in apoptosis control. Biochem Biophys Res Commun. 2005; 331:851–8. [PubMed: 15865941]
41. Vousden KH, Prives C. Blinded by the Light: The Growing Complexity of p53. Cell. 2009; 137:413–31. [PubMed: 19410540]
42. Yu Q, La Rose J, Zhang H, Takemura H, Kohn KW, Pommier Y. UCN-01 inhibits p53 up-regulation and abrogates gamma-radiation-induced G(2)-M checkpoint independently of p53 by targeting both of the checkpoint kinases, Chk2 and Chk1. Cancer research. 2002; 62:5743–8. [PubMed: 12384533]
43. Arlander SJH, Eapen AK, Vroman BT, McDonald RJ, Toft DO, Karnitz LM. Hsp90 inhibition depletes Chk1 and sensitizes tumor cells to replication stress. Journal of Biological Chemistry. 2003; 278:52572–7. [PubMed: 14570880]
44. Jarosz DF, Lindquist S. Hsp90 and environmental stress transform the adaptive value of natural genetic variation. Science. 2010; 330:1820–4. [PubMed: 21205668]
45. Porter JR, Fritz CC, Depew KM. Discovery and development of Hsp90 inhibitors: a promising pathway for cancer therapy. Curr Opin Chem Biol. 2010; 14:412–20. [PubMed: 20409745]
46. Peng Y, Chen L, Li C, Lu W, Chen J. Inhibition of MDM2 by hsp90 contributes to mutant p53 stabilization. The Journal of biological chemistry. 2001; 276:40583–90. [PubMed: 11507088]
47. Muller P, Hrstka R, Coomber D, Lane DP, Vojtesek B. Chaperone-dependent stabilization and degradation of p53 mutants. Oncogene. 2008; 27:3371–83. [PubMed: 18223694]

NIH-PA Author Manuscript

NIH-PA Author Manuscript

NIH-PA Author Manuscript

48. Li D, Marchenko ND, Schulz R, Fischer V, Velasco-Hernandez T, Talos F, et al. Functional inactivation of endogenous MDM2 and CHIP by HSP90 causes aberrant stabilization of mutant p53 in human cancer cells. Mol Cancer Res. 2011; 9:577–88. [PubMed: 21478269]

49. Leibowitz BJ, Qiu W, Liu H, Cheng T, Zhang L, Yu J. Uncoupling p53 Functions in Radiation-Induced Intestinal Damage via PUMA and p21. Mol Cancer Res. 2011; 9:616–25. [PubMed: 21450905]

50. Modi S, Stopeck A, Linden H, Solit D, Chandarlapaty S, Rosen N, et al. HSP90 Inhibition Is Effective in Breast Cancer: A Phase II Trial of Tanespimycin (17-AAG) Plus Trastuzumab in Patients with HER2-Positive Metastatic Breast Cancer Progressing on Trastuzumab. Clin Cancer Res. 2011; 17:5132–9. [PubMed: 21558407]

51. Sequist LV, Gettinger S, Senzer NN, Martins RG, Janne PA, Lilenbaum R, et al. Activity of IPI-504, a novel heat-shock protein 90 inhibitor, in patients with molecularly defined non-small-cell lung cancer. J Clin Oncol. 2010; 28:4953–60. [PubMed: 20940188]

NIH-PA Author Manuscript

NIH-PA Author Manuscript

NIH-PA Author Manuscript

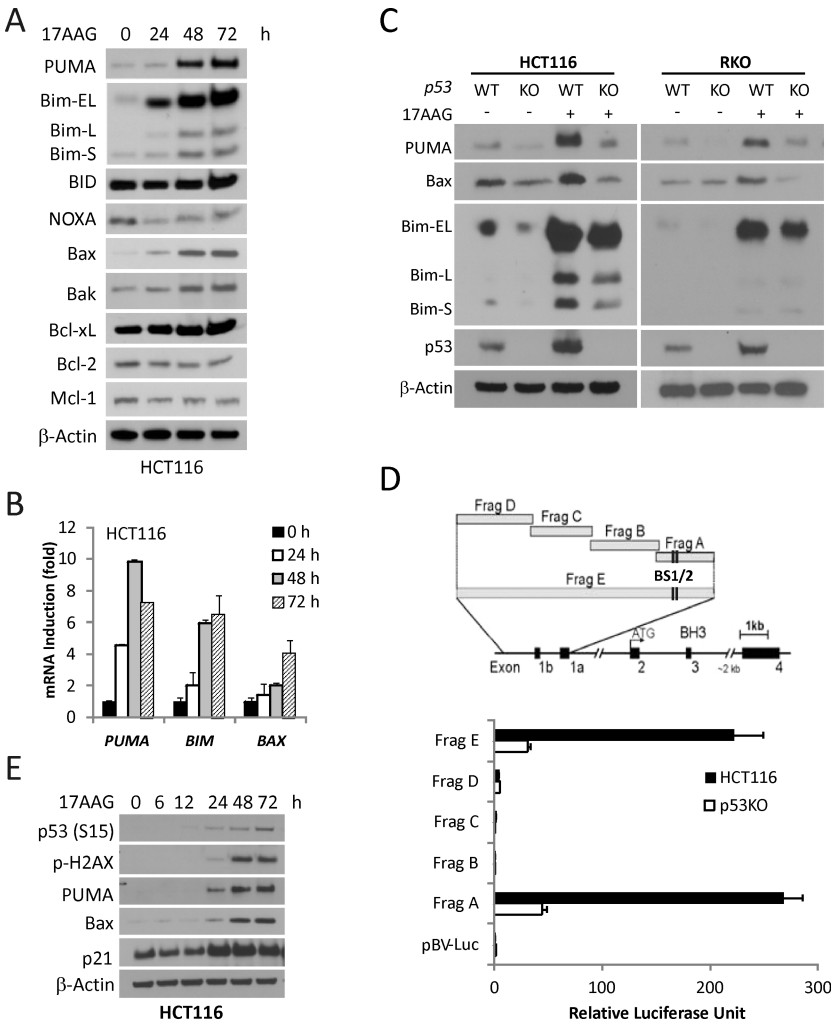

Figure 1. p53-dependent PUMA and Bax induction by 17AAG in colon cancer cells

Indicated cells were treated with 1 μM 17AAG and analyzed for protein or mRNA expression at indicated times. **(A)** The expression of Bcl-2 family members was analyzed by Western blotting. β-Actin was used as a loading control**. (B)** mRNA Levels of *PUMA, BIM, BAX* were analyzed by real-time reverse transcriptase (RT) PCR. *β-Actin* was used as a control. **(C)** WT and *p53*-KO HCT116 and RKO cells were treated with 1 μM 17AAG for 48 h. PUMA, Bim, Bax and p53 expression was analyzed by Western blotting. **(D)** Top, schematic representation of the genomic structure of *PUMA*, highlighting the *PUMA* promoter fragments A--E used in the luciferase experiment. Two p53 binding sites (BS1/2) are indicated by vertical lines. Bottom, WT and *p53*-KO HCT116 cells were transfected overnight with a luciferase reporter plasmids and then treated with 1 μM 17AAG for 24 h. Reporter activities were measured by luciferase assay. The ratios of normalized relative luciferase activities (to the empty vector pBV-Luc as 1) were plotted. (E) The indicated proteins were analyzed by Western blotting.

NIH-PA Author Manuscript
NIH-PA Author Manuscript
NIH-PA Author Manuscript

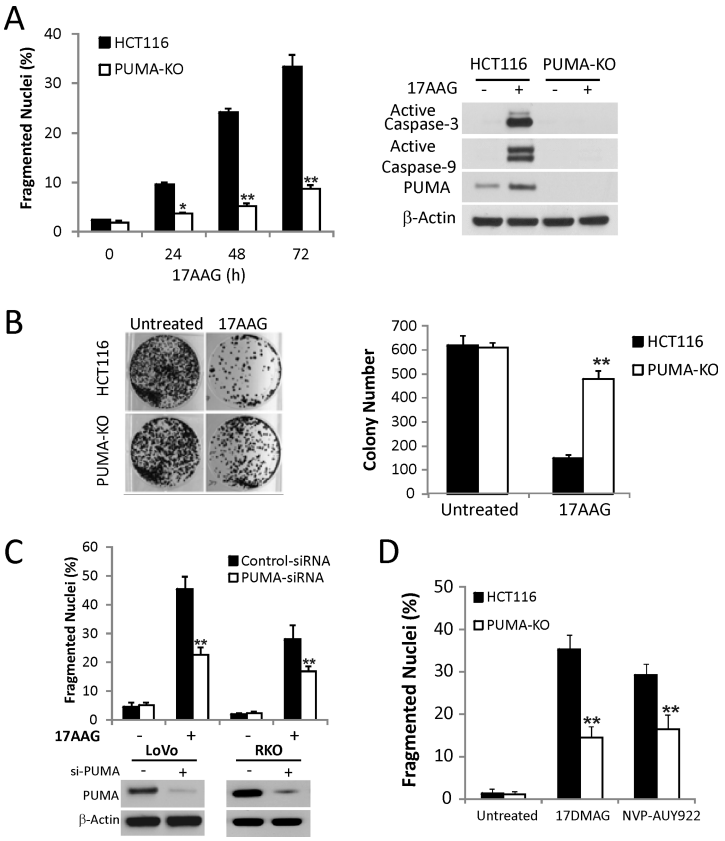

Figure 2. PUMA is required for Hsp90 inhibitor-induced apoptosis

(A) WT and *PUMA*-KO HCT116 cells were treated with 1 μM 17AAG. *Left*, apoptosis at the indicated times was analyzed for by counting condensed and fragmented nuclei. **, $P < 0.001$, WT *vs. PUMA*-KO. *Right*, Active caspase-3 and caspase-9 at 72 h were analyzed by Western blotting. **(B)** Colony formation assay was done by seeding an equal number of WT and *PUMA*-KO HCT116 cells treated with 1 μM 17AAG for 48 h in 12-well plates, and the attached cells were stained with crystal violet after 14 days. Representative pictures of colonies (Left) and quantification of colony numbers (Right) are shown. **, $P < 0.001$, WT *vs. PUMA*-KO. **(C)** LoVo and RKO cells were transfected with either a scrambled siRNA or *PUMA* siRNA for 24 h and then treated with 1 μM 17AAG for 48 h. *Top*, apoptosis was analyzed by counting condensed and fragmented nuclei. **, $P < 0.001$, si-PUMA *vs.* Scrambled. *Bottom*, Western blotting confirmed PUMA depletion by siRNA. **(D)** WT and *PUMA*-KO HCT116 cells were treated with 0.25 μM 17DMAG and 0.5 μM NVP-AUY922 for 48 h. Apoptosis was analyzed by counting condensed and fragmented nuclei. **, $P < 0.001$, WT *vs. PUMA*-KO.

NIH-PA Author Manuscript

NIH-PA Author Manuscript

NIH-PA Author Manuscript

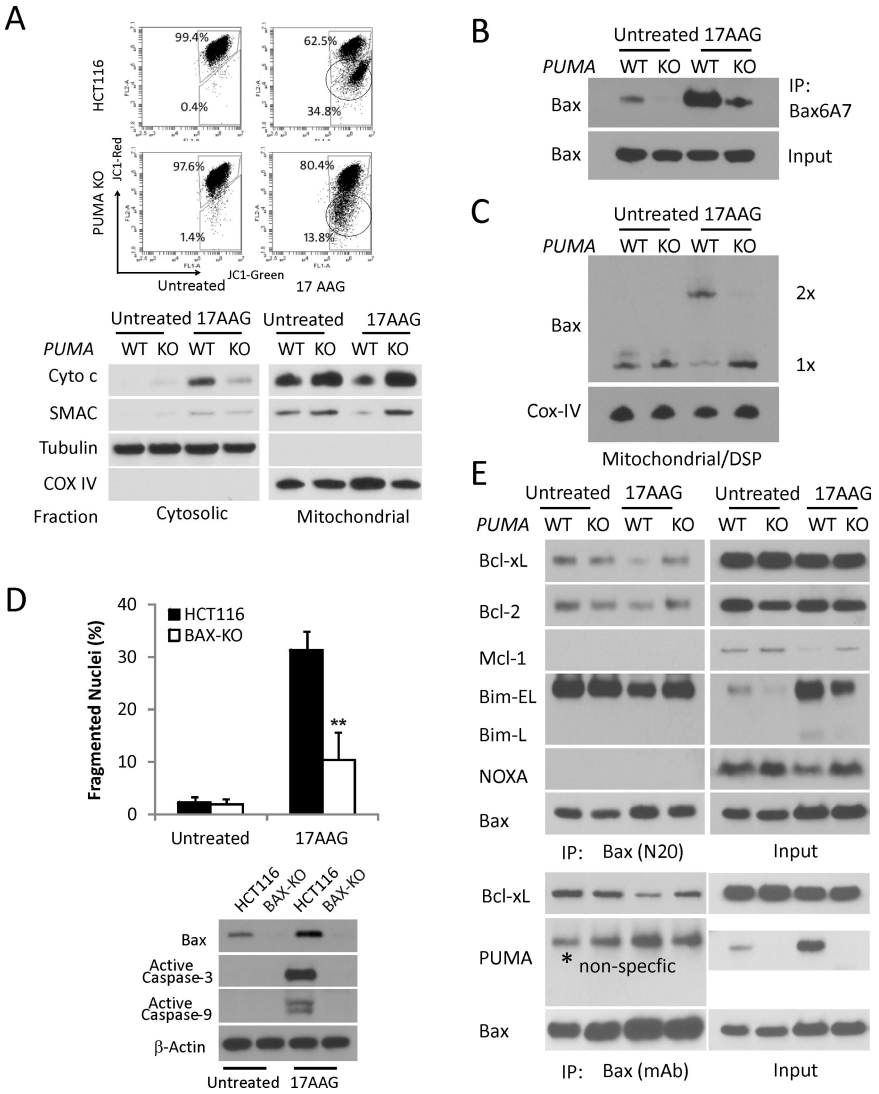

Figure 3. PUMA mediates 17AAG-induced apoptosis via the mitochondrial pathway and Bax activation in HCT116 cells

The indicated cells were treated with 1 μM 17AAG or vehicle (untreated) for 48 h. **(A)** *Upper,* mitochondrial membrane potential was analyzed by flow cytometry following staining with JC-1. The circled lower populations indicate decreased red/green ratio and membrane depolarization. *Lower,* the distribution of Cytochrome c and SMAC in mitochondrial or cytosolic fraction was analyzed by Western blotting. α-Tubulin and Cytochrome oxidase subunit IV (COX IV) were used as the control for fractionation. **(B)** Bax conformational change was detected by immunopercipiation (IP) with anti-Bax 6A7 (activated) antibody followed by Western blotting. **(C)** Bax multimerization in isolated mitochondria was analyzed by Western blotting under non-denaturing conditions following DSP crosslink. **(D)** Apoptosis was analyzed by counting condensed and fragmented nuclei (left) and Western blotting of active caspase-3, caspase-9 (lower). β-action was used as the control for loading. **(E)** Interactions of endogenous Bax with indicated Bcl-2 family members were analyzed by Immunoprecipitation (IP) followed by Western blotting. The Rabbit (N20, upper panels) and mouse (mAb, lower panels) anti-Bax antibodies were used.

NIH-PA Author Manuscript

NIH-PA Author Manuscript

NIH-PA Author Manuscript

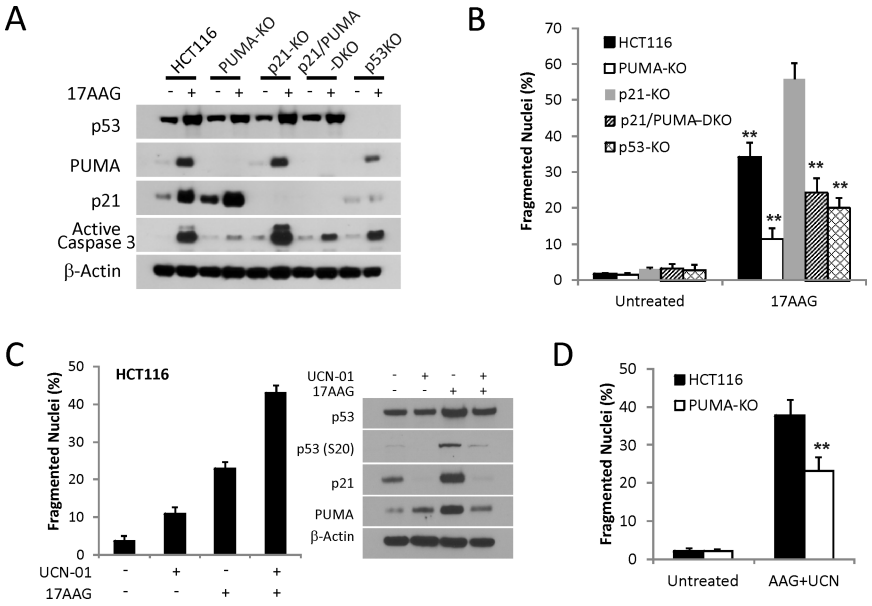

Figure 4. p53-dependent p21-induction suppresses 17AAG-induced apoptotic

(A) HCT 116 cell lines with the indicated genotypes were treated with 1 μM 17AAG for 48 h. Western blotting of PUMA, p21, p53 and active caspase-3. **(B)** Apoptosis was analyzed by counting condensed and fragmented nuclei in the indicated cell lines at 48 h. **, P < 0.001, *p21* KO *vs. WT, p53*-KO, *PUMA*-KO, or *p21/PUMA*-DKO. **(C)** HCT116 cells were treated with 1 μM UCN-01 or 1 μM 17AAG or their combination for 48 h. *Left,* apoptosis was analyzed by counting condensed and fragmented nuclei. *Right,* the expression levels of total p53, p-p53 (S20), p21 and PUMA were analyzed by Western blotting. **(D)** WT and *PUMA*-KO HCT116 cells were treated with 1 μM 17AAG and 1 μM UCN-01 for 48 h. Apoptosis was analyzed by counting condensed and fragmented nuclei. **, P < 0.001, WT *vs. PUMA*-KO.

NIH-PA Author Manuscript

NIH-PA Author Manuscript

NIH-PA Author Manuscript

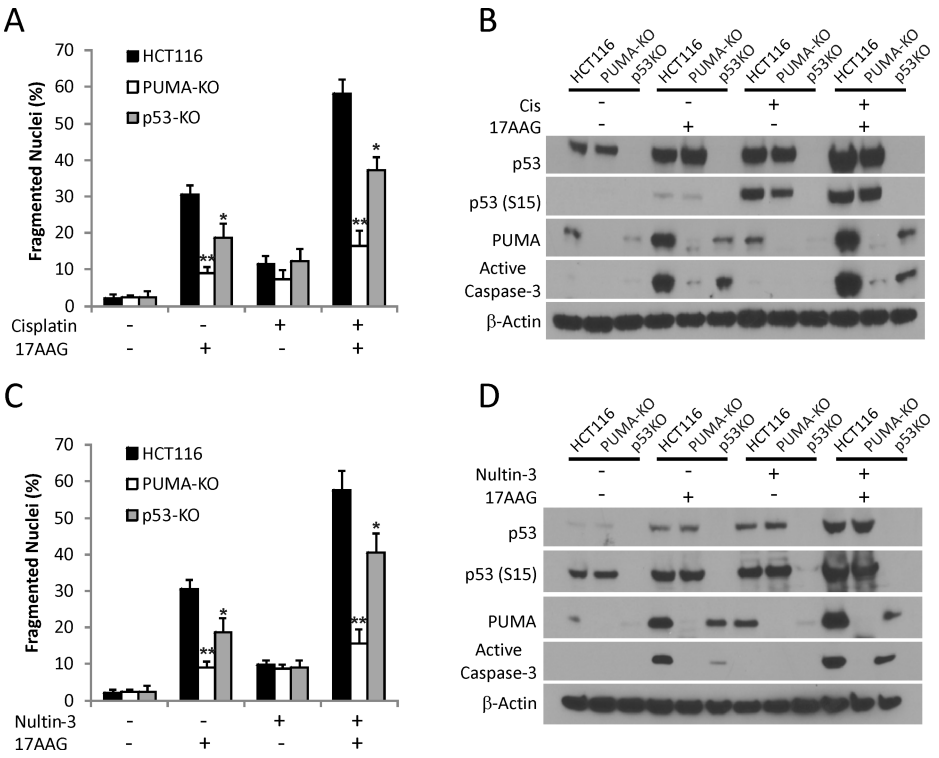

Figure 5. Enhanced p53 activity synergizes with 17AAG to induce PUMA and apoptosis

(A) WT, *PUMA*-KO and *p53*-KO HCT116 cells were treated with 1 μM 17AAG, 10 μM Cisplatin, or their combination for 48 h. Apoptosis was analyzed by counting condensed and fragmented nuclei. **(B)** Western blotting of active caspase-3, PUMA, p53 and p-p53 (S15) for samples in **(A). (C)** WT, *PUMA*-KO and *p53*-KO HCT116 cells were treated with 1 μM 17AAG or 10 μM Nutlin-3 or their combination for 48 h. Apoptosis was analyzed by counting condensed and fragmented nuclei. (**D)** Western blotting of active caspase-3, PUMA, phosphorylation of p53 on serine 15 for samples in **(C)**.

NIH-PA Author Manuscript

NIH-PA Author Manuscript

NIH-PA Author Manuscript

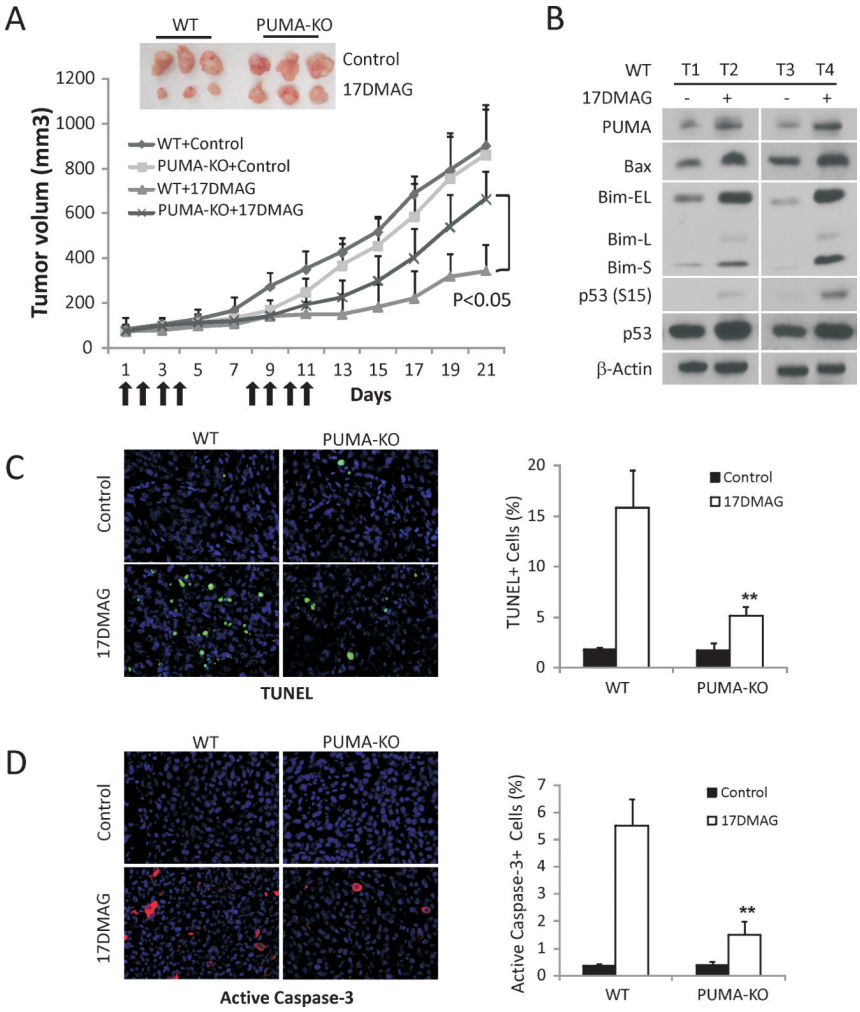

Figure 6. PUMA contributes to the anti-tumor activities of 17DMAG in a xenograft model

(A) Nude mice after 1 wk of implantation of 4×10^6 WT or *PUMA*-KO HCT116 cells were treated with 15 mg/kg of 17DMAG or the control buffer by i.p. injection on days 1-4 and 7-11. Tumor volume at indicated time points after treatment was calculated and plotted (n=6 in each group). *Top inset,* representative tumors at the end of the experiment. **(B)** HCT116 WT xenograft tumors from mice treated with 15 mg/kg of 17DMAG or the control buffer for five consecutive days. The indicated proteins were analyzed by Western blotting in representative tumors. **(C)** Paraffin-embedded WT and *PUMA*-KO tumor sections from mice treated as in **(B)** were analyzed by TUNEL staining. *Left*, representative TUNEL staining pictures; *Right*, TUNEL positive cells were counted and plotted. **(D)** Paraffin-embedded WT and *PUMA*-KO tumor sections from mice treated as in **(B)** were analyzed by active caspase-3 staining. *Left*, representative staining pictures. *Right*, active caspase-3 positive cells were counted and plotted.